

Seismic failure analysis and safety assessment of an extremely long-span transmission tower-line system

Li Tian^a, Haiyang Pan^b, Ruisheng Ma* and Xu Dong^c

School of Civil Engineering, Shandong University, Jinan, Shandong Province 250061, China

(Received October 24, 2018, Revised April 1, 2019, Accepted April 5, 2019)

Abstract. Extremely long-span transmission tower-line system is an indispensable portion of an electricity transmission system, and its failures or collapse can impact on the entire electricity grid, affect the modern life, and cause great economic losses. It is therefore imperative to investigate the failure and safety of the transmission tower subjected to ground motions. In the present study, a detailed finite element (FE) model of a representative extremely long-span transmission tower-line system is established. A segmental damage indicator (SDI) is proposed to quantitatively assess the damage level of each segment of the transmission tower under earthquakes. Additionally, parametric studies are conducted to investigate the influence of different ground motions and incident angles on the ultimate capacity and weakest segment of the transmission tower. Finally, the collapse fragility curve in terms of the maximum SDI value and PGA is plotted for the exemplified transmission tower. The results show that the proposed SDI can quantitatively assess the damage level of the segments, and thus determine the ultimate capacity and weakest segment of the transmission tower. Moreover, the different ground motions and incident angles have a significant influence on the SDI values of the transmission tower, and the collapse fragility curve is utilized to evaluate the collapse resistant capacity of the transmission tower subjected to ground motions.

Keywords: extremely long-span transmission tower-line system; failure analysis; segmental damage indicator; different ground motions; seismic incident angles; collapse fragility curve

1. Introduction

Due to the high dependencies on electricity, electricity transmission system has been widely recognized as a lifeline system. As a part of the entire system, the extremely long-span transmission tower-line systems will be constructed when the electricity transmission systems unavoidably cross great rivers or valleys. Compared to "ordinary" overhead transmission lines, the extremely long-span transmission tower-line system is generally more complicated due to its bigger height (over 100m) and larger spans (longer than 1000m). Additionally, the transmission tower-line system is inevitable to cover the regions with seismicity due to its great coverage.

Given these facts, the extremely long-span transmission tower-line system should be capable of resisting the failures during the earthquake. In the past decades, many research efforts have been dedicated to investigating the seismic responses of transmission tower-line system. Analytical studies were firstly conducted for the transmission tower-line system. In the analytical studies (Kempner and Smith 1984, Ghobarah *et al.* 1996, Li *et al.* 2005), the influence of the dynamic coupling effect of transmission lines and

spatially varying ground motions on the seismic responses of the transmission tower was preliminarily demonstrated. It should be noted that the analytical results are generally limited by the predefined assumptions in the analysis. To enhance the analysis accuracy, numerical simulation methods were subsequently introduced to investigate the seismic responses of transmission tower-line system (Wu *et al.* 2014, Tian *et al.* 2018b). In these studies, the effect of spatially varying excitations, near-fault ground motions and angles of incidence on the seismic responses of the transmission tower were demonstrated. Additionally, limited shaking table tests (Kotsubo *et al.* 1985, Tian *et al.* 2016a, Tian *et al.* 2017a) were also performed for the transmission tower-line system.

All the above researches demonstrated the seismic responses of the transmission tower-line system had been already investigated comprehensively. However, the failures of the transmission towers could still be observed in the past major earthquakes, such as the 1994 Northridge earthquake, the 1995 Kobe earthquake, the 1999 Chi-Chi earthquake and the 2008 Wenchuan earthquake (Hall *et al.* 1996, Shinozuka 1995, Chan *et al.* 2006; Xie and Zhu 2011). The failures of transmission tower-line systems not only result in economic losses but also impact the entire power grid net, hinder the relief after the earthquake. Considering these facts, the collapse (i.e. ultimate capacity) of the transmission tower has become an issue of interest in recent years. Albermani and Kitipornchai (2003) proposed a nonlinear analytical technique to evaluate the ultimate capacity of the transmission tower. A good match was found between the results obtained from the proposed method and

*Corresponding author, Ph.D.
E-mail: maruisheng@yeah.net

^a Professor

^b Ph.D. Student

^c M.Sc. Student

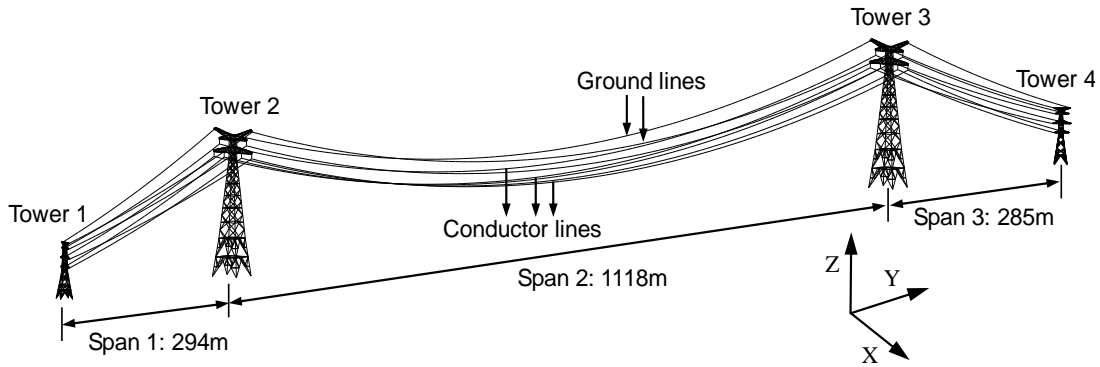


Fig. 1 Sketch of selected prototype

full-scale tower tests. Wang *et al.* (2013) developed a birth-to-death method to simulate the progressive collapse of the transmission tower-line systems subjected to severe earthquakes. It should be noted that this method is proposed based on an ideal elastic-plastic model without considering the nonlinear behaviors of members, such as yielding, buckling and post-buckling, etc. Considering the gaps, Tian *et al.* (2018a) proposed a new material model, dubbed Tian-Ma-Qu model, which could capture the nonlinear behaviors of steel tubes under axial cyclic loadings. This model was calibrated with the experimental results and had been utilized to simulate the collapse of transmission tower-line systems subjected to multi-component and near-fault seismic loadings (Tian *et al.* 2016b, Tian *et al.* 2017b). Similar to Tian-Ma-Qu model, an explicit dynamic analysis method was proposed in (Zheng *et al.* 2017, Zheng and Fan 2018, 2019) to model the progressive collapse of power transmission tower. Additionally, the element removal method (Asgarian *et al.* 2016) was also reported to assess the collapse fragility of the transmission tower. The critical literature review reveals that many studies have been completed to investigate the ultimate capacity or collapse of transmission tower-line system. However, no open studies are reported to quantitatively assess the damage of transmission tower subjected to ground motions.

To address the research gaps, a segmental damage indicator (SDI) is proposed to evaluate the damage for each segment of the transmission tower in the present study. This paper is organized as follows: Section 2 introduces the prototype and finite element model; Section 3 derives the segmental damage indicator for the transmission tower; Section 4 studies the collapse mechanism of the transmission tower, and performs parametric studies to investigate the influence of different ground motions and seismic incident angles on the ultimate capacity and weakest segment of the transmission tower; the collapse fragility curve of the transmission tower is developed in Section 5; Section 6 summarizes the major conclusions in the present study.

2. Prototype and finite element model

2.1 Selection of prototype

An extremely long-span transmission tower-line system crossing the Yellow River (the 2nd longest river in China) is

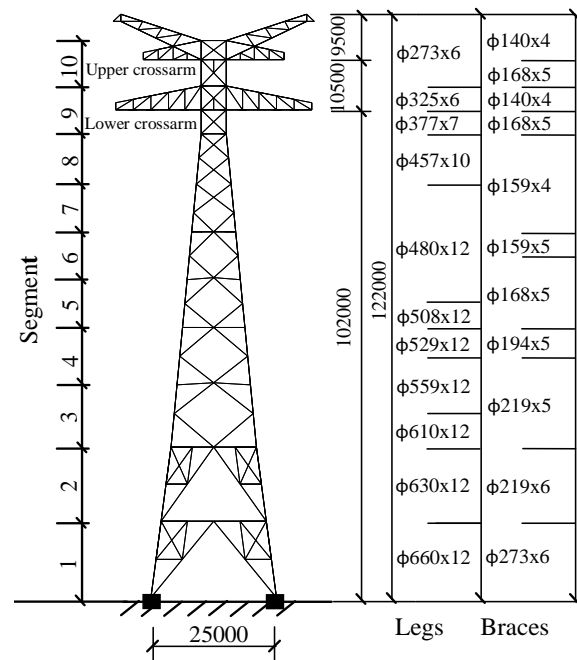


Fig. 2 Elevation of Towers 2 and 3 (unit: mm)

chosen as the prototype in the present study. This system is designed for the seismic hazard with the peak ground acceleration (PGA) of 0.2g, i.e. the exceeding probability of 10% in 50 years. Fig. 1 shows the sketch drawing of the selected transmission tower-line system. As shown, the selected prototype consists of four transmission towers (designated as Towers 1, 2, 3 and 4) and three spans of transmission lines (designated as Spans 1, 2 and 3). The lengths of Spans 1 to 3 are 294 m, 1118 m, 285 m, respectively, and the longest Span 2 crosses the Yellow River. In the original design, Towers 2 and 3 are the suspension-type tower supporting the transmission lines with vertical forces while Towers 1 and 4 are the tension-type tower providing tension forces. As mentioned above, this research focuses on the extremely long-span transmission tower. Additionally, the tension-type towers are generally designed with higher stiffness and lower height, which result in much smaller dynamic responses in Towers 1 and 4 in the comparison with Towers 2 and 3. As a result, Towers 2 and 3 are chosen as the primary objective of this research. It should be noted that Towers 2 and 3 have an identical design. As shown in Fig. 2, the tower has an

Table 1 Properties of conductor and ground lines

Category	Conductor line	Ground line
Designation	LHBGJ-400/95	OPGW-180
Total cross-section (mm ²)	501.02	175.2
Outside diameter (mm)	29.14	17.85
Elasticity modulus (GPa)	78000	170100
Coefficient of expansion (1/°C)	18.0E-6	12.0E-6
Mass per unit length (kg/km)	1856.7	1286

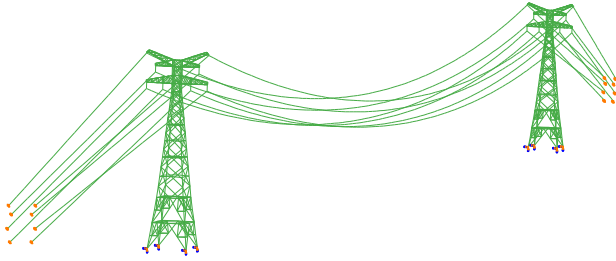


Fig. 3 FE model of the extremely long-span transmission tower-line system

overall height of 122m and a root span of 25m, and two cross arms are respectively mounted at the elevations of 102m and 112.5m. As shown, the detailed cross-section information is also given for the tower. It can be found that the tower consists of a series of steel tubes. These steel tubes are constructed by Q235 and Q345 steel. Furthermore, the tower body is divided into 10 segments (see Fig. 2) along the height of the tower. As for the transmission lines, conductor and ground wires respectively adopt LHBGJ-400/95 and OPGW-180 in the original design. The detailed properties of transmission lines are tabulated in Table 1. For convenience, the Cartesian coordinate system is introduced into the extremely long-span transmission tower-line system (see Fig. 1), and X, Y and Z axes denote the transverse, longitudinal and vertical directions of the system, respectively.

2.2 Finite Element Model

Based on the design information in Section 2, a detailed finite element (FE) model of the extremely long-span transmission tower system is established in the commercial software ABAQUS (version 6.12). Fig. 3 depicts the FE model which consists of two towers (i.e. Towers 2 and 3) and three spans of transmission lines. As mentioned in the prior section, Towers 2 and 3 are the principal objective in this research, and their responses are much smaller than those of Towers 1 and 4. Therefore, Towers 1 and 4 are omitted in the FE model for reducing the analysis cost. In the FE model, the transmission towers and lines are modeled by beam elements (B31) and truss elements (T3D2), respectively. There are a total of 1140 elements and 431 nodes in each transmission tower. For the transmission lines, the middle span (i.e. Span 2) and side spans (i.e. Spans 1 and 3) are respectively divided into 100 and 20

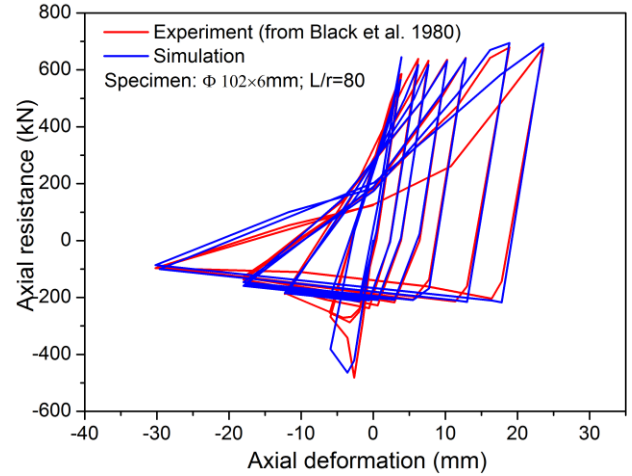


Fig. 4 Comparison between the experimental results and Tian-Ma-Qu model

elements to balance the analysis accuracy and cost. It is widely recognized that an ideal elastoplastic model is not enough accurate for nonlinear analyses since it cannot capture nonlinear behaviors, especially the buckling effect of steel members. Given this fact, the Tian-Ma-Qu material model is adopted for the transmission tower in this research. Fig. 4 gives the comparison between the experimental results and Tian-Ma-Qu model. It is found that this model has a fine match with the experimental result (Black *et al.* 1980), and can effectively capture the nonlinear behaviors of steel tubes under cyclic axial loadings. Interested readers can refer to (Tian *et al.* 2018a) for more detailed information. It should be noted that the damping ratios of transmission tower and lines are assumed to be 2% and 1%, respectively. Additionally, the gravity analysis will be conducted before the application of seismic excitations to determine the initial deformation of transmission lines.

Furthermore, the following damage index D is also introduced into the Tian-Ma-Qu model to calculate the damage for each member during analysis.

$$D = (1 - \beta_0) \frac{\varepsilon_m^p - \varepsilon_0^p}{\varepsilon_u^p - \varepsilon_0^p} + \beta_0 \sum_{k=1}^K \frac{\varepsilon_i^p - \varepsilon_0^p}{\varepsilon_u^p - \varepsilon_0^p} \quad (1)$$

where ε_0^p is the normal strain threshold value; ε_u^p is the ultimate normal strain of the material; ε_m^p is the maximum normal strain value during the analysis; ε_i^p is the highest normal strain during the i^{th} half loading cycle; N is the total number of half loading cycles; and β_0 is weight coefficient for the cumulative damage. In this damage model, “0” and “1” respectively denote the intact and fully damaged statuses of the member while the intermediate values between 0 and 1 represent the different damage level. More detailed information can be found in (Tian *et al.* 2018a).

3. Segmental damage indicator

In previous studies (e.g. (Tian *et al.* 2016b, Zheng *et al.* 2017)), the horizontal displacements at the top of the tower

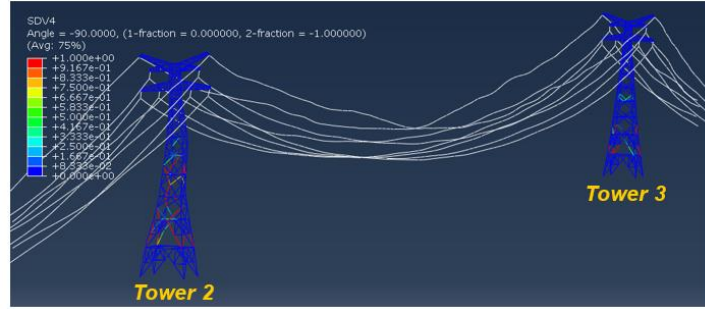


Fig. 5 Collapse of extremely long-span transmission tower-line system subjected to Imperial Valley wave (PGA=0.73g)

are generally utilized as an index to determine the states (i.e. collapse or non-collapse) of the transmission tower. However, this method may be not suitable for the extremely long-span transmission tower-line system subjected to ground motions. Compared to conventional buildings, the long-span transmission tower is more flexible and higher (122m for the prototype in this research). This means that the transmission tower may subject to a large rotational deformation which can increase the horizontal displacements at the top of the structure. There, it is not accurate to utilize the horizontal displacements at the top as a performance indicator. Additionally, the transmission tower can be considered consisting of many segments connected in series (see Fig. 2). This arrangement means that the overall damage level of the transmission tower can be determined by the maximum damage value of the segments. Therefore, a segmental damage indicator (SDI) is proposed to calculate the damage for each segment in the transmission tower. Given that there exist both parallel and series connections of members in each segment (see Fig. 2), the SDI is calculated by using the weighted mean method which has been widely applied in previous studies (Elenas 2000, Kostinakis *et al.* 2015, Barbosa *et al.* 2017). The SDI can therefore be expressed as follows:

$$SDI_i = \frac{\sum_{j=1}^n w_j D_j}{\sum_{j=1}^n w_j} \quad (2)$$

where D_j is the damage index of j th member in the i th segment and n is the total number of member in the j th segment; w_j is the weighting factor assigned to the j th member, which reflect the relative importance of the member in the overall structure. In many previous studies, the weighting factors are assumed to be proportional to the damage index D_j (Park *et al.* 1985, Powell and Allahabadi 1988, Williams and Sexsmith 1995). In other words, the member with a higher damage index has a more significant contribution to the overall damage of the segment. The Eq. (2) can be rewritten as

$$SDI_i = \frac{\sum_{j=1}^n D_j^2}{\sum_{j=1}^n D_j} \quad (3)$$

in which, D_j is the damage of j th member in i th segment, which can be calculated according to Eq. (1). After calculating the overall damage indicator, the next step is to classify the damage level of the segment. In practice, it is difficult to precisely define the damage level of structure.

Without the loss of generality, five damage levels of the segment are defined by referring to previous studies (Choi *et al.* 2004, Padgett and Desroches 2007, Han *et al.* 2014). These levels include the basically intact, slight damage, moderate damage, extensive damage and collapse. The corresponding threshold values are 0.2, 0.4, 0.6, and 0.8, respectively, and similar defined threshold values can be found in (Park *et al.* 1985, Niu and Ren 1991, Ghobarah *et al.* 1999).

4. Numerical studies and result discussions

In the prior section, the structural damage indicators (i.e. ODI and SDI) are derived for the transmission tower. In this section, the progressive collapse of the extremely long-span transmission tower-line system is investigated, and the proposed damage indicator, SDI, will be utilized to determine the critical PGA and weak positions of the structure. Note the critical PGA is defined as the peak ground acceleration corresponding to the onset of the collapse of the structure.

Additionally, the influence of different ground motions and seismic incident angles are also investigated. It should be noted that multi-component ground motions are considered in this section. Given the fact that the longitudinal direction of the transmission tower-line system is more adverse than transverse direction (Tian *et al.* 2018c), the horizontal component with larger PGA is applied along the longitudinal direction (Y axis) while another horizontal component is input along the transverse direction (X axis) of the transmission tower. The vertical component will be applied along the Z axis (see Fig. 1).

4.1 Collapse analysis of extremely long-span transmission tower-line system

In this subsection, a typical seismic record, namely Imperial Valley wave (El Centro Array #9, 1940), is utilized to investigate the collapse mechanism of the extremely long-span transmission tower-line system. To attain the collapse state of the transmission tower, incremental dynamic analysis (IDA) is carried out to determine the critical PGA of the Imperial Valley wave, which is equal to 0.73g. Fig. 5 illustrates the collapse of the extremely long-span transmission tower-line system subjected to Imperial Valley wave (PGA=0.73g). It should be noted that different colors represent the different damage level of members. The

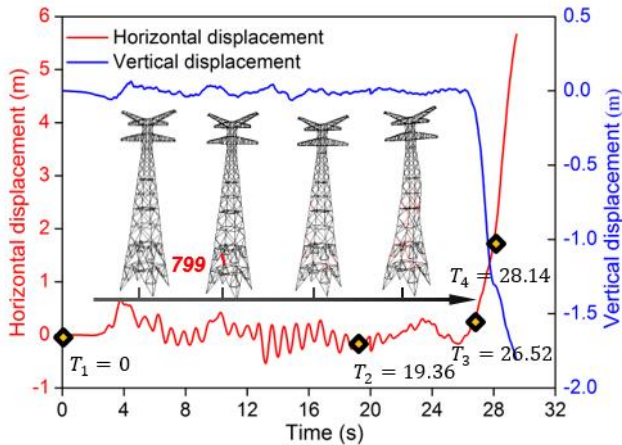


Fig. 6 Collapse process of Tower 2 subjected to Imperial Valley wave

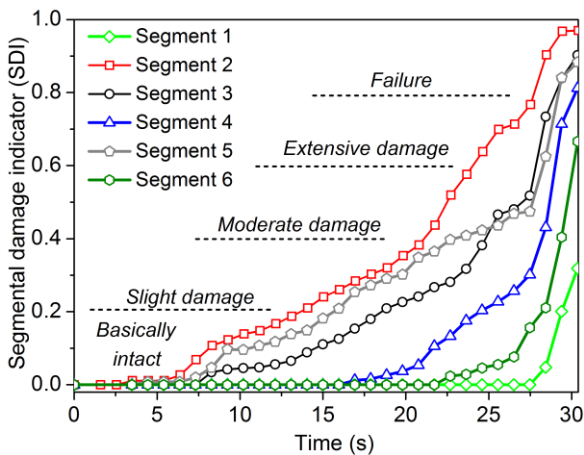


Fig. 7 SDI variation of Segments 1-6 in Tower 2

blue and red respectively denote the intact and completely failed of member, respectively. It can be found that the Tower 2 is damaged significantly and begins to collapse due to the massive failed members in Segments 2-5. Failed members are also found in Segments 2 and 3 of Tower 3. However, the damage extent of Tower 3 is much lower than that of Tower 2. This is because that the extremely long-span transmission tower-line system has different lengths in Spans 2 and 3 (see Fig. 1) which can result in different responses in these two towers. Owing to this fact, Tower 2 will be selected as the major objective in the following sections.

Fig. 6 shows the detailed collapse process of Tower 2 under Imperial Valley wave, and horizontal (Y direction) and vertical displacement time histories at the top of the tower. Additionally, four key time points (i.e. T_1 , T_2 , T_3 and T_4) and corresponding damage progression of Tower 2 are also given. It should be noted that the failed members are highlighted in red in the Figure. When the time t is less than T_2 (i.e. 19.36s), a few members are slightly damaged and no member fails. This means that the whole transmission tower is still almost elastic. As the time t increases to T_2 , the damage value D of a diagonal member (element No. 799) in Segment 2 reaches 1.0, which is the

Table 2 Summary of seismic wave records

ID	Event	Station	Year	Magnitude/M	PGA (g)
1	Kobe	Shin-Osaka	1995	6.9	0.240
2	Kern County	Taft Lincoln School	1952	7.36	0.180
3	Northridge	Villa Park-Serrano	1994	6.6	0.239

threshold value corresponding to the failure of the member. This indicates that this member is fully damaged and loses its bearing capacity. With the continuous input of ground motions, the number of failed members gradually increases. These failed members can lead to a local force redistribution, significantly increase the internal force of nearby members, and thus cause successive failures of members. When the time t reaches T_4 , a considerable number of members (including leg members, diagonal members and auxiliary members) fail and the entire transmission tower starts to collapse. At the same time, the displacement time histories in both the horizontal and vertical directions become unbounded.

Fig. 7 shows the SDI variation of different segments in Tower 2 subjected to Imperial Valley wave. It should be noted that only Segments 1-6 are shown in the Fig. since very slight damage can be found in Segments 7-10 (see Fig. 5). As shown, the SDI value of Segment 2 is always larger than those of other segments during the whole process, and firstly exceeds 0.8, namely the threshold value defined in Section 4. These facts indicate that Segment 2 is the relatively weak position for the exemplified transmission tower subjected to Imperial Valley wave. It is also found that the SDI values increase with the time t and the increasing extent grows significantly when the time t exceeds about 28s. This is because the failure of Segment 2 can trigger a rapid performance deterioration in the adjacent segments.

4.2 Influence of different ground motions

In the prior section, a typical seismic record (i.e. Imperial Valley wave) is adopted to investigate the collapse mechanism, collapse process and SDI variation of the extremely long-span transmission tower-line system. To consider the seismic uncertainties, the influence of different ground motions on the critical PGA and SDI values are further investigated in this subsection. Extra three seismic records are selected, and their detailed information can be found in Table 2.

Fig. 8 shows the SDI values of Segments 1-6 of the transmission tower subjected to different ground motions. The seismic record selected (i.e. Imperial Valley wave) in Section 4.1 is also presented here. The critical PGAs of different ground motions are also given in the Figure. It should be noted that only SDI values of Segments 1-6 are given here since those of other Segments (7-10) are much smaller. Additionally, in the Fig.8, the damage levels are not the final state of the segments (i.e. whole seismic duration) but the state corresponding to the first failure of segment. As shown, an obvious difference can be found between the critical PGAs (i.e. PGA_{cri} in the Figure) of different

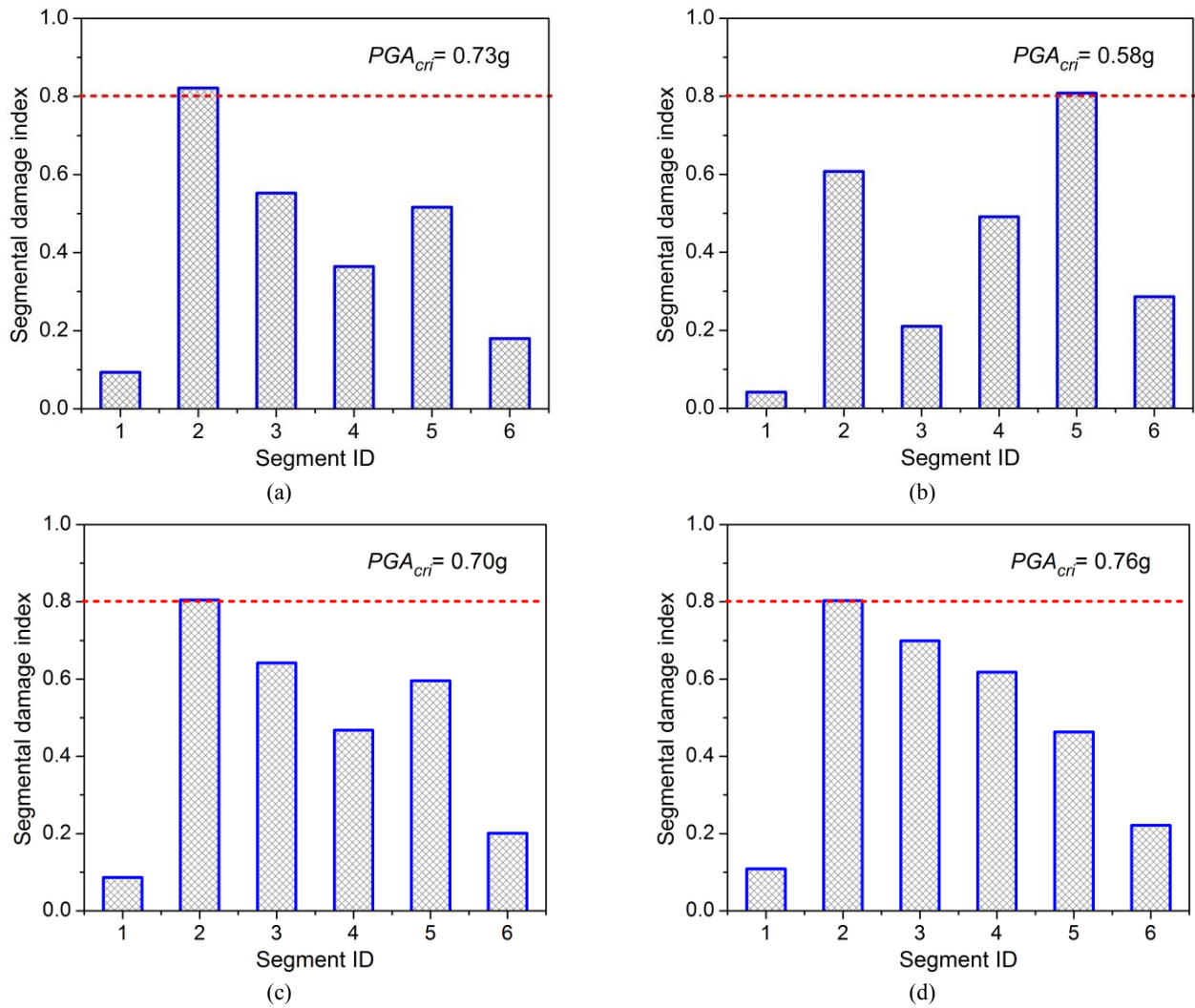


Fig. 8 SDI of Segments 1-6 of the transmission tower under different loading scenarios. (a) Imperial Valley; (b) Kobe; (c) Kern County; (d) Northridge

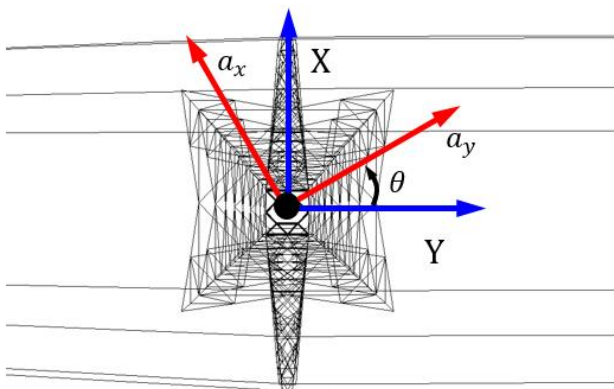


Fig. 9 Schematic diagram of seismic incident angles

seismic records. The maximum and minimum critical PGAs are 0.76g and 0.58g, respectively. This fact demonstrates that different ground motions have a great influence on the ultimate capacity of the extremely long-span transmission tower-line system. Similar results are also found for the “ordinary” transmission tower in (Zheng *et al.* 2017). It is also found that the SDI values do not follow a similar

variation trend in different loading scenarios. For Imperial Valley, Kern County and Northridge waves, the weakest segment of the transmission tower is Segment 2. However, for Kobe wave, the weakest segment is Segment 5 of the transmission tower. This indicates that the effect of different ground motions on the weakest segment cannot be ignored. All the above shows that the seismic uncertainties have a significant impact on the ultimate capacity and weakest position of the extremely long-span transmission tower-line system. Considering this fact, the collapse fragility analysis incorporating the seismic uncertainties will be conducted in Section 6.

4.3 Influence of seismic incident angle

In the prior sections, the horizontal components of each ground motion are applied along the X and Y axis of the FE model of extremely long-span transmission tower-line system (see Fig. 9). In other words, only one seismic incident angle is taken into account. However, the input direction of ground motion is not perfectly aligned with the longitudinal/transverse direction of the system in the

practice. This means that it is possible to underestimate the seismic demand of the transmission tower. Considering this fact, the influence of the seismic incident angles on the structural damage is investigated in this section. As shown in Fig. 19, the seismic incident angle θ is defined as the reference angle from the Y direction (i.e. the longitudinal direction of system) to the y_0 direction of seismic record, and assumed to be positive when it is counterclockwise. It should be noted that the y_0 direction denotes the horizontal component with a higher PGA while the x_0 direction represents another horizontal component of the seismic record. According to the Fig., the applied acceleration time histories along the X and Y directions of the long-span transmission tower-line system can be respectively expressed as follows

$$a_x(t) = a_x(t) \cos \theta + a_y(t) \sin \theta \quad (4a)$$

$$a_y(t) = a_y(t) \cos \theta - a_x(t) \sin \theta \quad (4b)$$

in which, $a_x(t)$ and $a_y(t)$ are the x-component and y-component acceleration time histories of seismic record. To determine the critical incident angle, the conventional method is to conduct a separated analysis for each possible angle of incidence. Obviously, this method is straightforward, but also significantly increases the computing cost of the analysis. To preclude the repetitive works, an effective approach is adopted to approximate the critical incident angle of the long-span transmission tower-line system. This method is quite simple and convenient to implement by utilizing the displacement spectra and modal information of the transmission towers, i.e. the natural periods and modal participation factors. Interested readers can find more detailed information in (Tian *et al.* 2018b). Table 3 tabulates the critical seismic incident angle of each ground motions. In the table, the corresponding critical PGAs of each ground motion at the critical and “ordinary” incident angles are also given. To clearly demonstrate the influence of critical incident angles, the following reduction ratio γ is introduced.

$$\gamma = \frac{(PGA_{cri} - PGA'_{cri})}{PGA_{cri}} \times 100\% \quad (5)$$

where, PGA_{cri} is the critical PGA of a ground motion with “ordinary” incident angle (i.e. 0° in this research); PGA'_{cri} is the critical PGA of a ground motions with the critical incident angle.

As shown, all the critical PGA values under critical incident angles are less than those under the ordinary incident angle, and all the reduction ratios are larger than 10%. These facts demonstrate that the seismic incident angles have an obvious effect on the ultimate capacity of the extremely long-span transmission tower-line system. Additionally, the critical incident angle varies with the ground motion. This is because the critical incident angle is calculated based on two parts: (1) displacement spectra of ground motions; (2) modal information of the transmission tower. Obviously, the modal information of the example transmission tower is deterministic while the displacement spectra will vary with each seismic record.

Table 3 Incident angle θ_{cri} and PGA_{cri} of different ground motions

Earthquake	Incident angles and PGA_{cri}				Reduction ratio γ (%)
	Critical incident angle θ_{cri} ($^\circ$)	PGA'_{cri} (g)	“Ordinary” incident angle ($^\circ$)	PGA_{cri} (g)	
Imperial Valley	115	0.65	0	0.73	11
Kobe	100	0.51	0	0.58	12
Kern County	45	0.63	0	0.70	10
Northridge	70	0.66	0	0.76	13

Fig. 10 gives the SDI values of Segments 1-6 of the extremely long-span transmission tower-line system under the critical incident angles. For comparison, the SDI values of Segment 1-6 of the system under the ordinary incident angle (i.e. 0°) is also given. It should be noted that the seismic PGAs of the ordinary incident angle are scaled to the critical PGAs of critical incident angles. As shown, the SDI values of the transmission tower under the critical incident angle are much larger than those under “ordinary” incident angle. Taken the Imperial Valley wave as an example, the SDI value of Segment 2 exceeds 0.8 (corresponding to “failure”) when the seismic incident angle is equal to 115° . However, under the ordinary incident angle (i.e. 0°), the SDI of Segment 2 is only about 0.4, corresponding to “moderate damage” as defined in Section 3. It is also found that the weakest segments (i.e. the segment with maximum SDI) are the same under the ordinary and critical incident angles. In summary, the critical incident angle has a significant influence on the ultimate capacity and damage level of the extremely long-span transmission tower-line system.

5. Collapse fragility analysis

As demonstrated above, the different ground motions have a significant influence on the critical PGA of extremely long-span transmission tower-line system. This means that the uncertainties of ground motions should be incorporated into the seismic safety assessment of the system. The fragility analysis is an effective and commonly utilized probabilistic approach to consider the seismic uncertainties. In this section, the collapse fragility curve of extremely long-span transmission tower-line system is plotted in terms of PGA and maximum SDI value. The seismic collapse fragility can be defined as the conditional probability that the structure will collapse when the seismic demand attaining or exceeding its ultimate capacity with a given intensity measure and described mathematically as follows:

$$P(C|IM = x) = P(S_d \geq d_u | IM = x) \quad (6)$$

where, $P(C|IM = x)$ is the structural collapse probability under a ground motion with a certain intensity measure (IM); S_d denotes the seismic demand measure (DM), i.e. the proposed SDI in this research; d_u is the

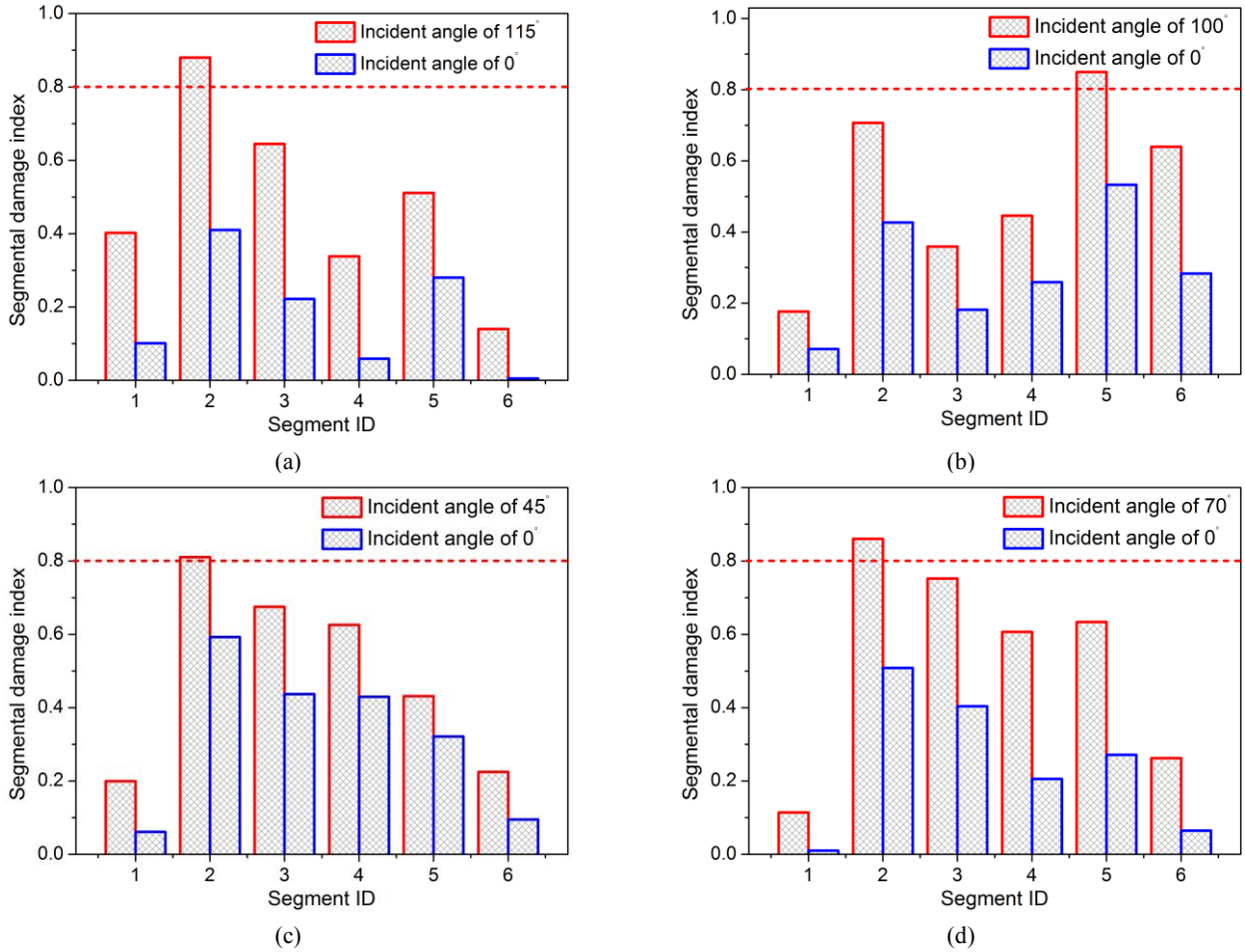


Fig. 10 Comparison of SDI values of the extremely long-span transmission tower-line subjected to ground motions with different incident angles. (a) Imperial Valley; (b) Borrego; (c) Kern County; (d) Northridge

threshold value corresponding to the collapse of the structure, which is taken as 0.8 as defined above.

Generally, a lognormal cumulative distribution assumption for IM (PGA) (Cornell *et al.* 2002) is utilized to define the fragility function:

$$P(C|IM = x) = \phi\left(\frac{\ln(PGA) - \ln \hat{\theta}}{\hat{\beta}}\right) \quad (7)$$

where, $\phi(\cdot)$ is the standard normal cumulative distribution function; $\hat{\theta}$ is the collapse median intensity (i.e., the PGA level with 50% probability of collapse), and $\hat{\beta}$ is standard deviation of the PGA. In addition, $\hat{\theta}$ and $\hat{\beta}$ can be computed by the following equations (Ibarra and Krawinkler 2005, Baker 2015)

$$\ln \hat{\theta} = \frac{1}{n} \sum_{k=1}^n \ln(PGA_k) \quad (8a)$$

$$a_y(t) = a_y(t) \cos \theta - a_x(t) \sin \theta \quad (8b)$$

where, n is the number of ground motions considered; PGA_k is the PGA value associated with the onset of collapse for the k_{th} ground motion.

To develop the collapse fragility curve, 20 far-field seismic records recommended by the Federal Emergency

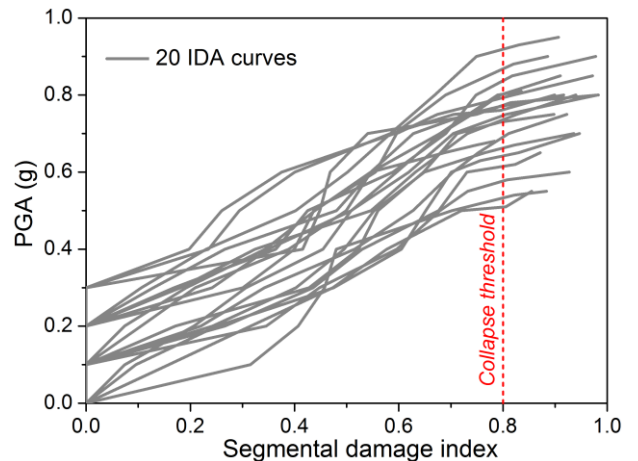


Fig. 11 IDA curves of 20 seismic records

Management Agency (FEMA) (FEMA-P695 2009) are selected in this research. The acceleration time histories of these selected ground motions are obtained from the databank of Pacific Earthquake Engineering Research Center (PEER). The detailed information of these selected seismic records can be found in Appendix A.

After the selection of seismic records, incremental dynamic analyses (IDAs) are carried out to generate enough

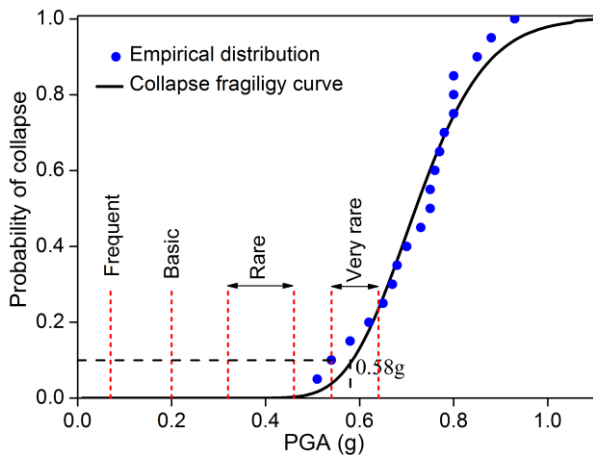


Fig. 12 Collapse fragility curve of extremely long-span transmission tower-line system

data for developing fragility curve. Fig. 11 shows the IDA curves of 20 far-field seismic records. As shown, the critical PGA of each seismic record is also given in the Figure. According to Eqs. 8 (a) and (b), the critical PGAs are utilized to calculate the $\hat{\theta}$ and $\hat{\beta}$, which are equal to 0.727 and 0.162, respectively.

Based on the IDA results and Eq. (7), the collapse fragility curve of the extremely long-span transmission tower-line system is plotted in Fig. 12. As mentioned above, the design PGA of this system is 0.2g, i.e. 10% probability of exceedance in 50 years. According to the seismic ground parameters zonation map of China (GB 18306-2015 2015), the PGAs of frequent, rare and very rare earthquakes (corresponding to the exceeding probabilities of 63.2% and 2% and 10⁻⁴ in one year, respectively) are 1/3, 1.6 to 2.3 times and 2.7 to 3.2 times of that of the basic earthquake. Thus, these PGA values are 0.067g, 0.32g to 0.46g and 0.54g to 0.64g, respectively. As shown in Fig. 12, the collapse probabilities of the extremely long-span transmission tower-line system under the frequent, basic and rare earthquake are zero, which indicate that this system is safe in these earthquakes. In other words, the transmission tower is designed with an adequate capacity to resist collapse in the frequent, basic and rare earthquakes. It is also found that the collapse probability of the system under very rare earthquake ranges from 0.038 to 0.236, which exceeds the recommended collapse threshold value of 10% in FEMA (FEMA-P695 2009). This fact demonstrates that the system is possible to fail when the very rare earthquake occurs.

6. Conclusions

This research focuses on the failure analysis of extremely long-span transmission tower-line system subjected to ground motions. A segmental damage indicator (SDI) is proposed to quantitatively assess the damage level of the segments of the transmission tower. Based on the proposed SDI, the ultimate capacity and weakest segment of the transmission tower are determined. Additionally, the influence of different ground motions and incident angles

are also investigated. Finally, the collapse fragility curve in terms of PGA and SDI is developed for the transmission tower subjected to ground motions. Based on the numerical results, the following significant conclusions can be drawn:

- The proposed segmental damage indicator (SDI) is capable of quantitatively assessing the damage level of the segments, determining the ultimate capacity and weakest segment of the transmission tower.
- Different ground motions can affect the ultimate capacity and weakest segment of the transmission tower, and the seismic uncertainties should be incorporated into the safety evolution of the structure.
- The seismic incident angle has a significant influence on the ultimate capacity and SDI values of the transmission tower. Ignoring the critical incident angle can overestimate the capacity of the transmission tower.

This extremely long-span transmission tower-line has adequate capacity to resist collapse in the frequent, basic and rare earthquakes, and is possible to collapse in the very rare earthquake.

Acknowledgements

This research was financially supported by the National Natural Science Foundation of China (Awards Nos. 51578325 and 51778347) and the Young Scholars Program of Shandong University (Awards No. 2017WLJH33).

References

- Albermani, F.G.A. and Kitipornchai, S. (2003), "Numerical simulation of structural behaviour of transmission towers", *Thin Walled Struct.*, **41**(2-3), 167-177. [https://doi.org/10.1016/S0263-8231\(02\)00085-X](https://doi.org/10.1016/S0263-8231(02)00085-X).
- Asgarian, B., Eslamlou, S.D., Zaghi, A.E. and Mehr, M. (2016), "Progressive collapse analysis of power transmission towers", *J. Constr. Steel Res.*, **123**, 31-40. <https://doi.org/10.1016/j.jcsr.2016.04.021>.
- Baker, J.W. (2015), "Efficient analytical fragility function fitting using dynamic structural analysis", *Earthq. Spectra*, **31**(1), 579-599. <https://doi.org/10.1193/021113EQS025M>.
- Barbosa, A.R., Ribeiro, F.L.A. and Neves, L.A.C. (2017), "Influence of earthquake ground-motion duration on damage estimation: application to steel moment resisting frames", *Earthq. Eng. Struct. D.*, **46**(1), 27-49. <https://doi.org/10.1002/eqe.2769>.
- Black, R.G., Wenger, W.A. and Popov, E.P. (1980), *Inelastic Buckling of Steel Struts Under Cyclic Load Reversals, UCB/EERC-80/40*, Earthquake Engineering Research Center, Berkeley, CA, USA.
- Chan, Y.F., Alagappan, K., Gandhi, A., Donovan, C., Tewari, M. and Zaets, S.B. (2006), "Disaster management following the Chi-Chi earthquake in Taiwan", *Prehosp. Disaster med.*, **21**(3), 196-202. <https://doi.org/10.1017/S1049023X00003678>.
- Choi, E., Desroches, R. and Nielson, B. (2004), "Seismic fragility of typical bridges in moderate seismic zones", *Eng. Struct.*, **26**(2), 187-199. <https://doi.org/10.1016/j.engstruct.2003.09.006>.
- Cornell, C.A., Jalayer, F., Hamburger, R.O. and Foutch, D.A. (2002), "Probabilistic basis for 2000 SAC federal emergency management agency steel moment frame guidelines", *J. Struct. Eng.*, **128**(4), 526-533. [https://doi.org/10.1061/\(ASCE\)0733-9445\(2002\)128:4\(526\)](https://doi.org/10.1061/(ASCE)0733-9445(2002)128:4(526)).

- Elenas, A. (2000), "Correlation between seismic acceleration parameters and overall structural damage indices of buildings", *Soil. Dyn. Earthq. Eng.*, **20**(1), 93-100. [https://doi.org/10.1016/S0267-7261\(00\)00041-5](https://doi.org/10.1016/S0267-7261(00)00041-5).
- FEMA-P695 (2009), Quantification of Building Seismic Performance Factors, Applied Technology Council; Washington, DC, USA.
- GB 18306-2015 (2015), Seismic Ground Motion Parameters Zonation Map of China, Standardization Administration of China Press; Beijing, China.
- Ghobarah, A., Aziz, T.S. and El-Attar, M. (1996), "Response of transmission lines to multiple support excitation", *Eng. Struct.*, **18**(12), 936-946. [https://doi.org/10.1016/S0141-0296\(96\)00020-X](https://doi.org/10.1016/S0141-0296(96)00020-X).
- Ghobarah A., Abou-Elfath H. and Biddah A. (1999), "Response-based damage assessment of structures", *Earthq. eng. struct.*, **28**(1): 79-104. [https://doi.org/10.1002/\(SICI\)1096-9845\(199901\)28:1%3C79::AID-EQE805%3E3.0.CO;2-J](https://doi.org/10.1002/(SICI)1096-9845(199901)28:1%3C79::AID-EQE805%3E3.0.CO;2-J).
- Hall, J.F., Holmes, W.T. and Somers, P. (1996), "Northridge earthquake, January 17, 1994", Earthquake Engineering Research Institute, California, USA.
- Han, R., Li, Y. and Lindt, J.V.D. (2014), "Seismic risk of base isolated non-ductile reinforced concrete buildings considering uncertainties and mainshock-aftershock sequences", *Struct. Saf.*, **50**, 39-56. <https://doi.org/10.1016/j.strusafe.2014.03.010>.
- Ibarra, L.F. and Krawinkler, H. (2005), *Global Collapse of Frame Structures under Seismic Excitations*, Pacific Earthquake Engineering Research Center Berkeley, CA, USA.
- Kempner Jr, L. and Smith, S. (1984), "Cross-ropes transmission tower-line dynamic analysis", *J. Struct. Eng.*, **110**(6), 1321-1335. [https://doi.org/10.1061/\(ASCE\)0733-9445\(1984\)110:6\(1321\)](https://doi.org/10.1061/(ASCE)0733-9445(1984)110:6(1321)).
- Kostinakis, K., Athanopoulou, A. and Morfidis, K. (2015), "Correlation between ground motion intensity measures and seismic damage of 3D R/C buildings", *Eng. Struct.*, **82**, 151-167. <https://doi.org/10.1016/j.engstruct.2014.10.035>.
- Kotsubo, S., Takanishi, T., Uno, K. and Sonoda, T. (1985), "Dynamic tests and seismic analysis of high towers of electrical transmission line", *Transactions of the Japan society of civil engineers*, **15**, 72-75.
- Li, H.N., Shi, W.L., Wang, G.X. and Jia, L.G. (2005), "Simplified models and experimental verification for coupled transmission tower-line system to seismic excitations", *J. Sound Vib.*, **286**(3), 569-585. <https://doi.org/10.1016/j.jsv.2004.10.009>.
- Niu, D.T. and Ren, L.J. (1996), "A modified seismic damage model with double variables for reinforced concrete structures", *Earthq. Eng. Eng. Vib.*, **16**(4), 44-54.
- Padgett, J.E. and Desroches, R. (2007), "Bridge Functionality Relationships for Improved Seismic Risk Assessment of Transportation Networks", *Earthq. Spectra*, **23**(1), 115-130. <https://doi.org/10.1193/1.2431209>.
- Park, Y.J., Ang, A.H.S. and Wen, Y.K. (1985), "Seismic damage analysis of reinforced concrete buildings", *J. Struct. Eng.*, **111**(4), 740-757. [https://doi.org/10.1061/\(ASCE\)0733-9445\(1985\)111:4\(740\)](https://doi.org/10.1061/(ASCE)0733-9445(1985)111:4(740)).
- Powell, G.H. and Allahabadi, R. (1988), "Seismic damage prediction by deterministic methods: concepts and procedures", *Earthq. Eng. Struct. D.*, **16**(5), 719-734. <https://doi.org/10.1002/eqe.4290160507>.
- Shinozuka, M. (1995), "The Hanshin-Awaji earthquake of January 17, 1995 Performance of life lines", Report NCEER-95-0015, NCEER. <http://hdl.handle.net/10477/757>.
- Tian, L., Gai, X. and Qu, B. (2017a), "Shake table tests of steel towers supporting extremely long-span electricity transmission lines under spatially correlated ground motions", *Eng. Struct.*, **132**, 791-807. <https://doi.org/10.1016/j.engstruct.2016.11.068>.
- Tian, L., Gai, X., Qu, B., Li, H.N. and Zhang, P. (2016a), "Influence of spatial variation of ground motions on dynamic responses of supporting towers of overhead electricity transmission systems: An experimental study", *Eng. Struct.*, **128**, 67-81. <https://doi.org/10.1016/j.engstruct.2016.09.010>.
- Tian, L., Ma, R.S., Li, H.N. and Wang, Y. (2016b), "Progressive collapse of power transmission tower-line system under extremely strong earthquake excitations", *J. Struct. Stab. D.*, **16**(1), 1-21. <https://doi.org/10.1142/S0219455415500303>.
- Tian, L., Ma, R.S. and Qu, B. (2018a), "Influence of different criteria for selecting ground motions compatible with IEEE 693 required response spectrum on seismic performance assessment of electricity transmission towers", *Eng. Struct.*, **156**, 337-350. <https://doi.org/10.1016/j.engstruct.2017.11.046>.
- Tian, L., Ma, R.S., Qiu, C.X., Xin, A.Q., Pan, H.Y. and Guo, W. (2018c), "Influence of multi-component ground motions on seismic responses of long-span transmission tower-line system: An experimental study", *Earthq. Struct.*, **15**(6), 583-593. <https://doi.org/10.12989/eas.2018.15.6.583>.
- Tian, L., Pan, H.Y., Ma, R.S. and Qiu, C.X. (2017b), "Collapse simulations of a long span transmission tower-line system subjected to near-fault ground motions", *Earthq. Struct.*, **13**(2), 211-220. <https://doi.org/10.12989/eas.2017.13.2.211>.
- Tian, L., Yi, S.Y. and Qu, B. (2018b), "Orienting ground motion inputs to achieve maximum seismic displacement demands on electricity transmission towers in near-fault regions", *J. Struct. Eng.*, **144**(4). [https://doi.org/10.1061/\(ASCE\)ST.1943-541X.0002000](https://doi.org/10.1061/(ASCE)ST.1943-541X.0002000).
- Wang, W.M., Li, H.N. and Tian, L. (2013), "Progressive collapse analysis of transmission tower-line system under earthquake", *Adv. Steel Constr.*, **9**(2), 161-172.
- Williams, M.S. and Sexsmith, R.G. (1995), "Seismic damage indices for concrete structures: a state-of-the-art review", *Earthq. Spectra*, **11**(2), 319-349. <https://doi.org/10.1193/1.1585817>.
- Wu, G., Zhai, C.H., Li, S. and Xie, L. (2014), "Effects of near-fault ground motions and equivalent pulses on large crossing transmission tower-line system", *Eng. Struct.*, **77**, 161-169. <https://doi.org/10.1016/j.engstruct.2014.08.013>.
- Xie, Q. and Zhu, R. (2011), "Earth, wind, and ice", *IEEE Power Energy M.*, **9**(2), 28-36. <https://doi.org/10.1109/MPE.2010.939947>.
- Zheng, H.D. and Fan, J. (2018), "Analysis of the progressive collapse of space truss structures during earthquakes based on a physical theory hysteretic model", *Thin Walled Struct.*, **123**, 70-81. <https://doi.org/10.1016/j.tws.2017.10.051>.
- Zheng, H.D., Fan, J. and Long, X.H. (2017), "Analysis of the seismic collapse of a high-rise power transmission tower structure", *J. Constr. Steel Res.*, **134**, 180-193. <https://doi.org/10.1016/j.jcsr.2017.03.005>.
- Zheng, H.D. and Fan, J. (2019), "Phenomenological hysteretic model for steel braces including inelastic postbuckling and low-cycle fatigue prediction", *J. Struct. Eng.*, **145**(6), [https://doi.org/10.1061/\(ASCE\)ST.1943-541X.0002319](https://doi.org/10.1061/(ASCE)ST.1943-541X.0002319).

Appendix A

No.	Earthquake			PGA (g)	Recording station
	Name	Magnitude/M	Year		
1	San Fernando	6.6	1971	0.21	LA-Hollywood Stor
2	Friuli, Italy	6.5	1976	0.35	Tolmezzo
3	Imperial Valley	6.5	1979	0.35	Delta
4	Imperial Valley	6.5	1979	0.38	El Centro Array #11
5	Superstition Hills	6.5	1987	0.36	El Centro Imp. Co.
6	Loma Prieta	6.9	1989	0.53	Capitola
7	Loma Prieta	6.9	1989	0.56	Gilroy Array #3
8	Landers	7.3	1992	0.24	Yermo Fire Station
9	Landers	7.3	1992	0.42	Coolwater
10	Cape Mendocino	7.0	1992	0.55	Rio Dell Overpass
11	Northridge	6.7	1994	0.52	Beverly Hills-Mulhol
12	Northridge	6.7	1994	0.48	Canyon Country-WLC
13	Kobe, Japan	6.9	1995	0.51	Nishi-Akashi
14	Kobe, Japan	6.9	1995	0.24	Shin-Osaka
15	Duzce, Turkey	7.1	1999	0.82	Bolu
16	Hector Mine	7.1	1999	0.34	Hector
17	Kocaeli, Turkey	7.5	1999	0.36	Duzce
18	Kocaeli, Turkey	7.5	1999	0.22	Arcelik
19	Chi-Chi, Taiwan	7.6	1999	0.44	CHY101
20	Chi-Chi, Taiwan	7.6	1999	0.51	TCU045